Chapter 7

Modeling of cellular layers

String L-systems, the first formalism considered in this book, are suitable for the modeling of nonbranching filaments such as *Anabaena catenula*. The introduction of brackets extends the class of modeled structures to axial trees. However, many structures found in botany have a more complex topology, which can only be described by graphs with cycles. The developmental surface models presented in Section 5.2 make it possible to specify a limited class of these graphs. This chapter describes a more general approach and applies it to simulate the development of single-layered cellular structures such as those found in fern gametophytes, animal embryos and plant epidermis. All structures considered are of microscopic dimensions and relatively undifferentiated, yet the presented methods may bring us closer to the modeling of more complex patterns, such as the venation of leaves.

The modeling method consists of two stages. First, the *topology* of the cell division patterns are expressed using the formalism of *map L-systems*, which allows for the formation of cycles in a structure. At this stage the neighborhood relations between cells are established, but the cell shapes remain unspecified. Next, cell *geometry* is modeled using a dynamic method that takes into account the osmotic pressure inside the cells and the tension of cell walls. The development can be animated by considering periods of continuous cell expansion, delimited by instantaneous cell divisions.

7.1 Map L-systems

From a mathematical perspective, cellular layers can be represented using a class of planar graphs with cycles, called *maps* [148]. Nakamura *et al.* [102] characterize them as follows:

Maps as models of cell layers

- A map is a finite set of *regions*. Each region is surrounded by a boundary consisting of a finite, circular sequence of *edges* that meet at *vertices*.

- Each edge has one or two vertices associated with it. The one-vertex case occurs when an edge forms a loop. The edges cannot cross without forming a vertex and there are no vertices without an associated edge.

- Every edge is a part of the boundary of a region.

- The set of edges is connected. Specifically, there are no islands within regions.

A map corresponds to a microscopic view of a cellular layer. Regions represent cells, and edges represent cell walls perpendicular to the plane of view. The internal components of a cell are not considered.

Map rewriting   The process of cell division can be described by map rewriting. This notion is an extension of string rewriting as discussed in Section 1.2. In general, map-rewriting systems are categorized as *sequential* or *parallel*, and can be *region-controlled* or *edge-controlled* [87]. Since several cells may divide concurrently, a parallel rewriting system is needed. The second categorization has to do with the form of rewriting rules, which may express cell subdivisions in terms of region labels or edge labels. Both approaches are suitable for biological modeling purposes [22]. This chapter focuses on the edge-controlled formalism of *Binary*

mBPMOL-   *Propagating Map OL-system with markers*, or mBPMOL-systems. It
systems   was proposed by Nakamura, Lindenmayer and Aizawa [102] as a refinement of the basic concept of map L-systems introduced by Lindenmayer and Rozenberg [91]. The name is derived as follows. A *map OL-system* is a parallel rewriting system that operates on maps and does not allow for interaction between regions. In other words, regions are modified irrespective of what happens to neighboring regions (a *context-free* mechanism). The system is *binary* because a region can split into at most two daughter regions. It is *propagating* in the sense that the edges cannot be erased, thus regions (cells) cannot fuse or die. The *markers* specify the positions of inserted edges that split the regions.

The choice of mBPMOL-systems as a modeling tool has two justifications. First, they are more powerful than other interactionless map-rewriting systems described in the literature [19, 22, 23]. In addition, markers have a biological counterpart in preprophase bands of microtubules, which coincide with the attachment sites for division walls formed during mitosis [55]. It should be noted, however, that *double wall* systems, introduced by J. and H. B. Lück [93], may be relatively easier to specify [23].

Definition   An mBPMOL-system $\mathcal{G}$ consists of a finite alphabet of *edge labels* Σ, a *starting map* ω with labels from Σ, and a finite set of *edge productions* P. In general, the edges are *directed*, which is indicated by a left or right arrow placed above the edge symbol. In some cases, the edge direction has no effect on the system operation. Such an edge is called *neutral* and no arrow is placed above the symbol denoting it. Each production is of the form $A \to \alpha$, where the directed or neutral

a

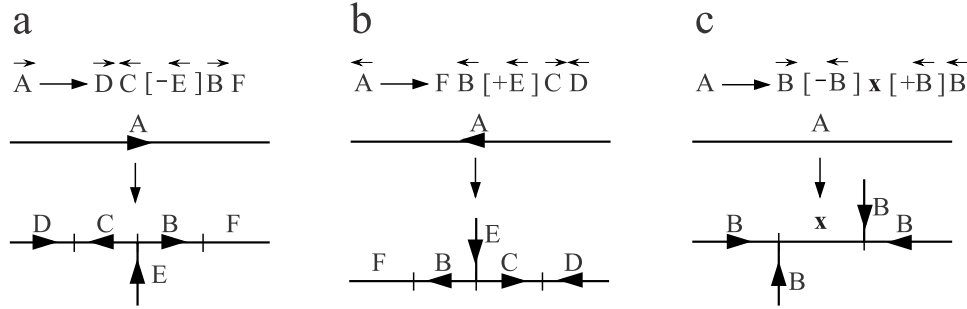$\vec{A} \longrightarrow \vec{D}\,\overset{\rightarrow}{\underset{}{C}}[-\overleftarrow{E}]\,\vec{B}\,F$

b

$\overleftarrow{A} \longrightarrow F\,\overleftarrow{B}\,[+\overleftarrow{E}]\,\overset{\rightarrow}{\underset{}{C}}\,\overleftarrow{D}$

c

$A \longrightarrow \vec{B}\,[-\overleftarrow{B}]\,\mathbf{x}\,[+\overleftarrow{B}]\,\overleftarrow{B}$

Figure 7.1: Examples of edge productions

edge $A \in \Sigma$ is called the *predecessor*, and the string α, composed of symbols from Σ and special symbols $[,], +,$ and $-$, is called the *successor*. The symbols outside square brackets specify the edge subdivision pattern. Arrows can be placed above edge symbols to indicate whether the successor edges have directions consistent with, or opposite to, the predecessor edge. Pairs of matching brackets $[$ and $]$ delimit *markers*, which specify possible attachment sites for region-dividing walls. The markers are viewed as short branches that can be connected to form a complete wall. The strings inside brackets consist of two symbols. The first symbol is either $+$ or $-$, indicating whether the marker is placed to the left or to the right of the predecessor edge. The second symbol is the marker label, with or without an arrow. The left arrow indicates that the marker is directed towards the predecessor edge, and the right arrow indicates that the marker is directed away from that edge. If no arrow is present, the marker is neutral.

Production syntax

For example, in the production $\vec{A} \to \vec{D}\overleftarrow{C}[-\overleftarrow{E}]\vec{B}F$, the directed predecessor A splits into four edges D, C, B and F, and produces a marker E (Figure 7.1a). Successor edges D and B have the same direction as A, edge C has the opposite direction, and F is neutral. Marker E is placed to the right of A and is directed towards A. Note that this same production could be written as $\overleftarrow{A} \to F\overleftarrow{B}[+\overleftarrow{E}]\vec{C}\overleftarrow{D}$ (Figure 7.1b). As an example of a production with a neutral predecessor, consider $A \to \vec{B}[-\overleftarrow{B}]x[+\overleftarrow{B}]\overleftarrow{B}$. In this case the result of production application does not depend on the assumed direction of the predecessor edge (Figure 7.1c).

A *derivation step* in an mBPMOL-system consists of two phases.

Derivation

- Each edge in the map is replaced by successor edges and markers using the corresponding edge production in P.

- Each region is scanned for *matching markers*.

$$
\begin{aligned}
\omega &: & \texttt{ABAB} \\
p_1 &: & \texttt{A} &\rightarrow \texttt{B[-A][+A]B} \\
p_2 &: & \texttt{B} &\rightarrow \texttt{A}
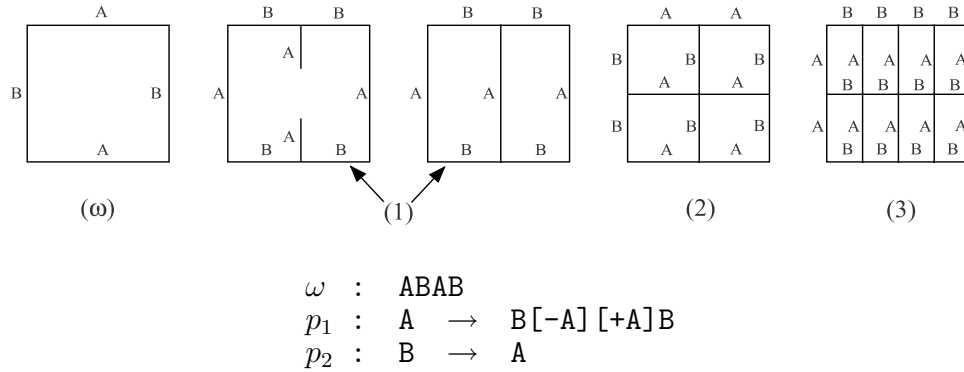\end{aligned}
$$

Figure 7.2: Example of a map L-system. In the first step, a distinction is made between the edge-rewriting phase and the connection of matching markers.

Two markers are considered matching if:

- they appear in the same region,

- they have the same label, and

- one marker is directed away from its incident edge while the other is directed towards the edge, or both markers are neutral.

If a match is found, the markers are joined to create a new edge that will split the region. The search for matching markers ends with the first match found, even though other markers entering the same region may also form a match. From the user's perspective, the system behaves nondeterministically since it chooses the pair of markers to be connected. The unused markers are discarded.

Examples   The operation of mBPMOL-systems is illustrated in the following examples. The L-system shown in Figure 7.2 has two productions. Production p_1 creates markers responsible for region division, while production p_2 introduces a delay needed to subdivide the regions alternately by horizontal and vertical edges.

The L-system shown in Figure 7.3 is a modified version of the previous one. The only difference is the addition of an edge x, which separates the markers in the successor of production p_1. This edge creates a Z-shaped offset between the inserted edges A. Z-offsets and symmetric S-offsets (Figure 7.4) can be observed in many biological structures [22, 92].

Figure 7.5 illustrates the operation of an mBPMOL-system with directed edges. Productions p_1 and p_3 create markers. Production p_4

$$
\begin{array}{ll}
\omega & : \quad \texttt{ABAB} \\
p_1 & : \quad \texttt{A} \quad \rightarrow \quad \texttt{B[-A]x[+A]B} \\
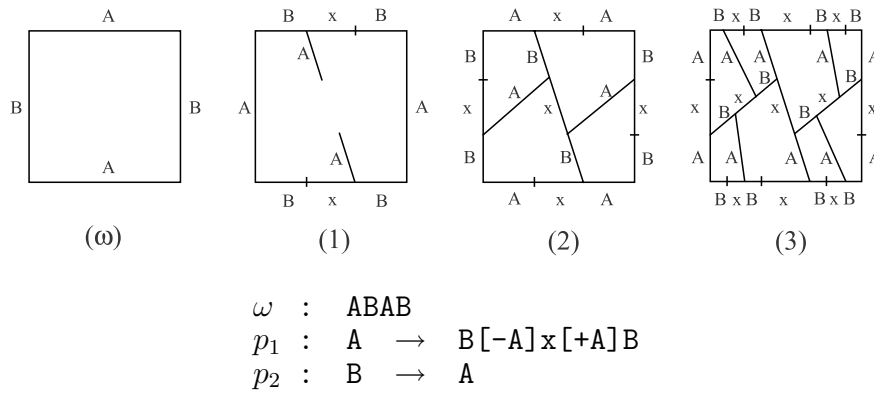p_2 & : \quad \texttt{B} \quad \rightarrow \quad \texttt{A}
\end{array}
$$

Figure 7.3: Example of a map L-system

Figure 7.4: Offsets between four regions that result from the division of two regions sharing a common edge: (a) Z-offset, (b) S-offset
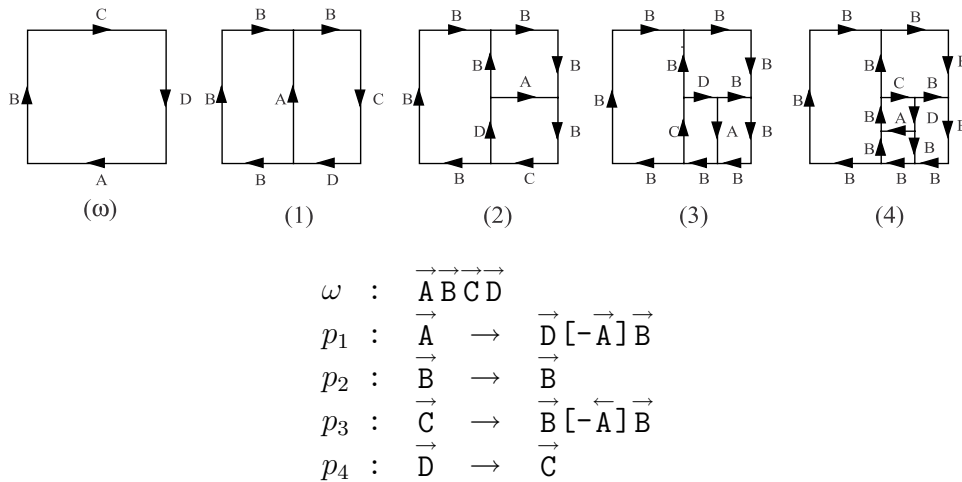

$$
\begin{array}{ll}
\omega & : \quad \overrightarrow{\texttt{A}}\,\overrightarrow{\texttt{B}}\,\overrightarrow{\texttt{C}}\,\overrightarrow{\texttt{D}} \\
p_1 & : \quad \overrightarrow{\texttt{A}} \quad \rightarrow \quad \overrightarrow{\texttt{D}}\,\texttt{[}{-}\overrightarrow{\texttt{A}}\texttt{]}\,\overrightarrow{\texttt{B}} \\
p_2 & : \quad \overrightarrow{\texttt{B}} \quad \rightarrow \quad \overrightarrow{\texttt{B}} \\
p_3 & : \quad \overrightarrow{\texttt{C}} \quad \rightarrow \quad \overrightarrow{\texttt{B}}\,\texttt{[}{-}\overleftarrow{\texttt{A}}\texttt{]}\,\overrightarrow{\texttt{B}} \\
p_4 & : \quad \overrightarrow{\texttt{D}} \quad \rightarrow \quad \overrightarrow{\texttt{C}}
\end{array}
$$

Figure 7.5: Example of a map L-system with directed edges

transforms edge D into C, so that in each derivation step there is a pair of edges A and C to which productions p_1 and p_3 apply. Production p_2 indicates that edges B do not undergo further changes.[1] The resulting structure is that of a clockwise spiral.

7.2   Graphical interpretation of maps

Maps are topological objects without inherent geometric properties. In order to visualize them, some method for assigning geometric interpretation must be applied. In its description, the biologically-motivated terms *cell* and *wall* will be used instead of their mathematical counterparts, region and edge.

Wall subdivision   Siero, Rozenberg and Lindenmayer [131] proposed a method that, in the simplest case, is expressed by the following rules:

- walls are represented by straight lines,

- the starting map is represented by a regular polygon, bounded by the walls specified in the axiom,

- when a production subdivides a wall, all successor walls are of equal length, and

- the position of a wall resulting from the union of two matching markers is based on the position of these markers.

This *wall subdivision* method was used to draw Figures 7.2, 7.3 and 7.5. However, in a biological context it creates cells with shapes that are seldom observed in nature.

Center of gravity method   De Does and Lindenmayer [24] proposed a *center of gravity* method that produces more realistic shapes. According to this method each interior vertex of the map is placed at the center of gravity of its neighbors. Such positioning of vertices has a sound biological justification; it minimizes hypothetical forces acting along cell walls, thus bringing the entire structure to a state of minimum energy. However, if all vertices were positioned this way, the entire structure would collapse. To counteract this effect, the vertices on the map perimeter are displaced outward a fixed distance. Unfortunately, this lacks biological justification and introduces sudden shape changes after cell divisions have occurred, making it unsuitable for animation purposes.

Dynamic method   Assuming a dynamic point of view, the shape of cells and thus the shape of the entire organism results from the action of forces. The unbalanced forces due to cell divisions cause the gradual modification of cell shapes until an equilibrium is reached. At this point, new cell divisions occur, and the search for an equilibrium resumes.

---

[1]In further L-systems such identity productions are omitted.

The dynamic method is based on the following assumptions:

- the modeled organism forms a single cell layer,

- the layer is represented as a two-dimensional network of masses corresponding to cell vertices, connected by springs that correspond to cell walls,

- the springs are always straight and obey Hooke's law,

- each cell exerts pressure on its bounding walls directly proportional to the wall length and inversely proportional to the cell area,

- the pressure on a wall is divided evenly between the wall vertices,

- the motion of masses is damped, and

- no other forces (for example, due to friction or gravity) are considered.

The position of each vertex, and thus the shape of the layer, is computed as follows. As long as an equilibrium is not reached, unbalanced forces put masses in motion. The total force $\vec{F}_T$ acting on a vertex X is given by the formula

$$\vec{F}_T = \sum_{w \in W} \vec{F}_w + \vec{F}_d,$$

where $\vec{F}_w$ are forces contributed by the set W of walls w incident to X, and $\vec{F}_d = -b\vec{v}$ is a damping force, expressed as the product of a damping factor b and vertex velocity $\vec{v}$.

A wall $w \in W$ contributes three forces acting on X (Figure 7.6). The *tension* $\vec{F}_s$ acts along the wall, and its magnitude is determined by Hooke's law,

$$\vec{F}_s = -k(l - l_0),$$

where k is the spring constant, l is the current spring length, and l_0 is its rest length. The remaining forces, $\vec{P}_L$ and $\vec{P}_R$, are due to the *pressure* exerted by the cells on the left and right sides of the wall. Each force acts in a direction perpendicular to the wall and is distributed equally between the incident vertices. The magnitude of these forces equals $p \cdot l$, where p is the internal cell pressure and l is the wall length. The pressure is assumed to be inversely proportional to the cell area: $p \sim A^{-1}$. This assumption is derived from the equation describing osmotic pressure, $p = SRT$, as a function of the concentration of the solute S (n moles per volume V), the ideal gas constant R, and the absolute temperature T [129]. Assuming that the cell volume V is
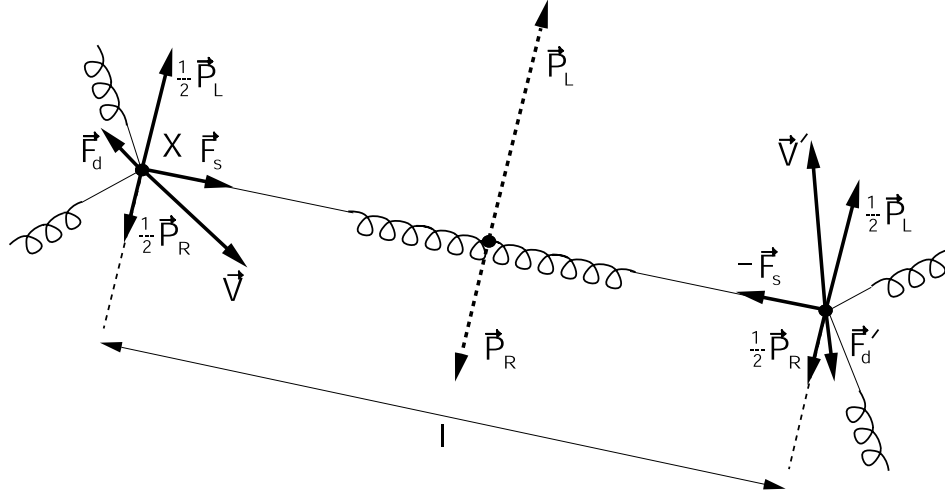
Figure 7.6: Forces acting on a cell vertex X

proportional to the area A captured by the two-dimensional model under consideration ($V = Ah$), pressure can be expressed as

$$p = \frac{nRT}{Ah}.$$

Thus $p \sim A^{-1}$, provided that the term nRT/h is constant. A convenient formula for calculating the area A is

$$A = |\sum_{i=1}^{M} (x_i - x_{i+1})(y_i + y_{i+1})/2|,$$

where (x_i, y_i) are coordinates of the M vertices of the cell, $x_{M+1} = x_1$, and $y_{M+1} = y_1$.

The force $\vec{F}_T$ acts on a mass placed at a map vertex. Newton's second law of motion applies,

$$m\frac{d^2\vec{x}}{dt^2} = \vec{F}_T,$$

where $\vec{x}$ is the vertex position. If the entire structure has N vertices, a system of $2N$ differential equations is obtained,

$$m_i\frac{d\vec{v}_i}{dt} = \vec{F}_{T_i}(\vec{x}_1, \cdots, \vec{x}_N, \vec{v}_i)$$
$$\frac{d\vec{x}_i}{dt} = \vec{v}_i,$$

where $i = 1, 2, \ldots, N$. The task is to find the sequence of positions $\vec{x}_1, \ldots, \vec{x}_N$ at given time intervals, assuming that the functions $\vec{F}_{T_i}$ and the initial values of all variables $\vec{x}_1^0, \ldots, \vec{x}_N^0$ and $\vec{v}_1^0, \ldots, \vec{v}_N^0$ are known. These initial values are determined as follows.

- Coordinates of the vertices of the starting map are included in the input data for the simulation.

- Positions of existing vertices are preserved through a derivation step. New vertices partition the divided walls into segments of equal length. The initial velocities of all vertices are set to zero.

The system of differential equations with the initial values given above represents an *initial value problem*. It can be solved numerically using the *forward (explicit) Euler method* [41]. To this end, the differential equations are rewritten using finite increments $\Delta \vec{v}_i$, $\Delta \vec{x}_i$ and Δt,

$$\Delta \vec{v}_i^k = \frac{1}{m_i} \vec{F}_{T_i} \left(\vec{x}_1^k, \cdots, \vec{x}_N^k, \vec{v}_i^k \right) \Delta t$$
$$\Delta \vec{x}_i^k = \vec{v}_i^k \Delta t,$$

where the superscripts $k = 0, 1, 2, \ldots$ indicate the progress of time, $t = k\Delta t$. The position and velocity of a point i after time increment Δt are expressed as follows:

$$\vec{v}_i^{k+1} = \vec{v}_i^k + \Delta \vec{v}_i^k$$
$$\vec{x}_i^{k+1} = \vec{x}_i^k + \Delta \vec{v}_x^k$$

The iterative computation of the velocities $\vec{v}_i^k$ and positions $\vec{x}_i^k$ is carried out for consecutive values of index k until all increments $\Delta \vec{v}_i$ and $\Delta \vec{x}_i$ fall below a threshold value. This indicates that the equilibrium state has been approximated to the desired accuracy. The next derivation step is then performed. A system of equations corresponding to the resulting map is created, and the search for an equilibrium state resumes. In this way, the developmental process is simulated as periods of continuous cell expansion, delimited by instantaneous cell divisions. Continuity of cell shapes during divisions is preserved by the rule that sets the initial positions of vertices.

For example, Figure 7.7 illustrates the expansion of a structure generated by the L-system specified in Figure 7.3 in a derivation of length 4. Figure 7.7a shows the structure immediately after the insertion of division walls, Figures 7.7b and c present intermediate wall positions, and Figure 7.7d describes the final structure at equilibrium.

7.3   Microsorium linguaeforme

In this section, the described simulation method is applied to visualize the development of the fern gametophyte *Microsorium linguaeforme*. The biological data is based on observations conducted by de Boer [22]. Fern gametophytes represent the sexually reproducing life stage of fern
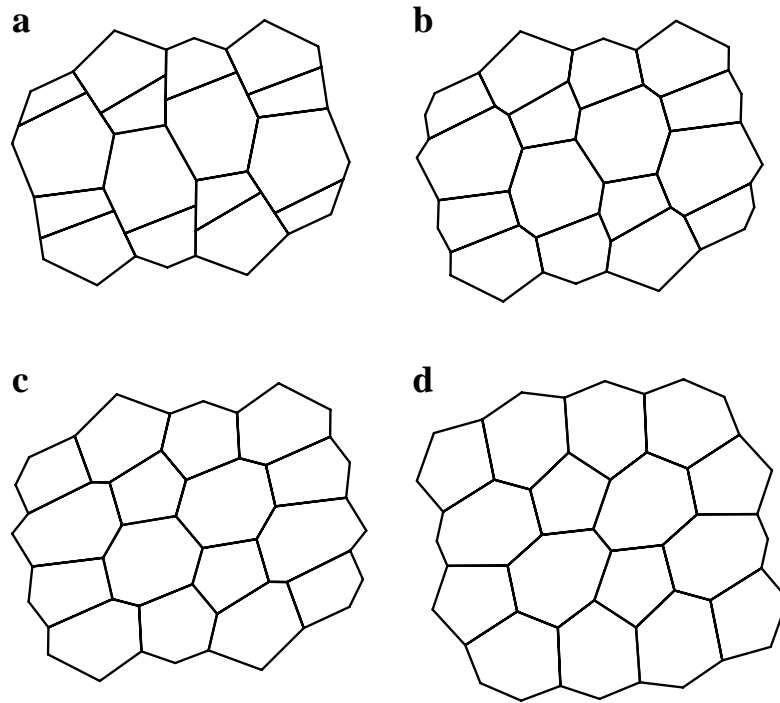
a

b

c

d

Figure 7.7: Expansion of a cellular structure: (a) after division, (b) and (c) intermediate positions, (d) equilibrium

plants. They show no differentiation into stem, leaf and root, forming a plant body called a *thallus*. The development of a thallus can be described conveniently in terms of the activity of the *apical cell* giving rise to *segments*, and the development of these segments. The modeling process captures repetitive patterns of cell divisions, so that large cellular structures can be described using a small number of productions.

Apical activity   The apical cell is the originator of the gametophyte structure. It divides repetitively, giving rise each time to a new apical cell and a primary (initial) segment cell. The segment cells subsequently develop into multicellular segments. The division wall of an apical cell is attached to the thallus border on one side and to a previously created division wall on the other side. Thus, the division walls are oriented alternately to the left and to the right, yielding two columns of segments separated by a zig-zag dividing line (Figure 7.8). The recursive nature of the apical activity can be expressed by the following formula (called a *cell division system* [22]):

$$A_L \rightarrow S_L \mid A_R \qquad\qquad A_R \rightarrow A_L \mid S_R$$

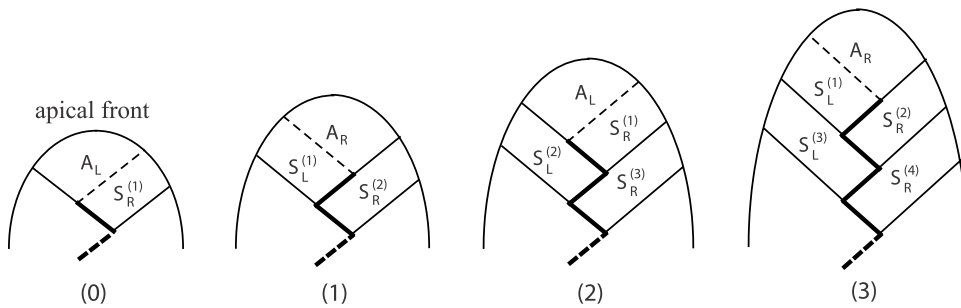This notation means that the cell on the left side of the arrow produces two daughter cells separated by a wall.

Figure 7.8: Apical production of segments. The labels A_R and A_L denote apical cells producing right segment S_R and left segment S_L, respectively. Dashed lines indicate the newly created division wall. The superscripts represent segment age. The internal structure of segments is not shown.
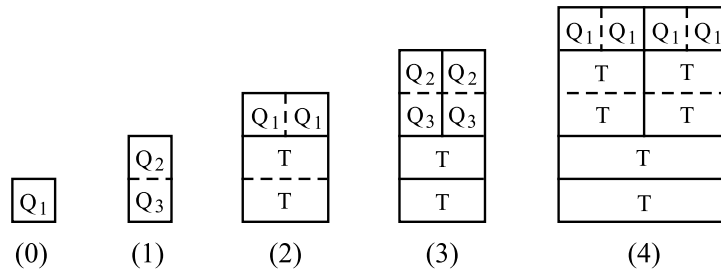

Figure 7.9: Developmental sequence of a *Microsorium* segment

In describing the structure of a segment, we distinguish between *periclinal* and *anticlinal* walls. Intuitively, periclinal walls are approximately parallel to the *apical front* of the thallus, and anticlinal walls are perpendicular to this front. A more formal definition follows.

Division pattern of segments

- In a primary segment, the apical front wall and one or more walls opposing it are periclinal walls. The remaining walls are anticlinal walls.

- A division wall attached to two periclinal walls is an anticlinal wall, and vice-versa.

In *Microsorium*, a wall is never attached to a periclinal wall on one side and an anticlinal wall on the other side, so the above definition comprises all possible cases.

Microscopic observations of growing *Microsorium* gametophytes reveal that most segments follow the same developmental sequence, shown diagrammatically in Figure 7.9. The primary segment cell Q_1 is first divided by a periclinal wall into two cells, Q_2 and Q_3. Subsequently, the
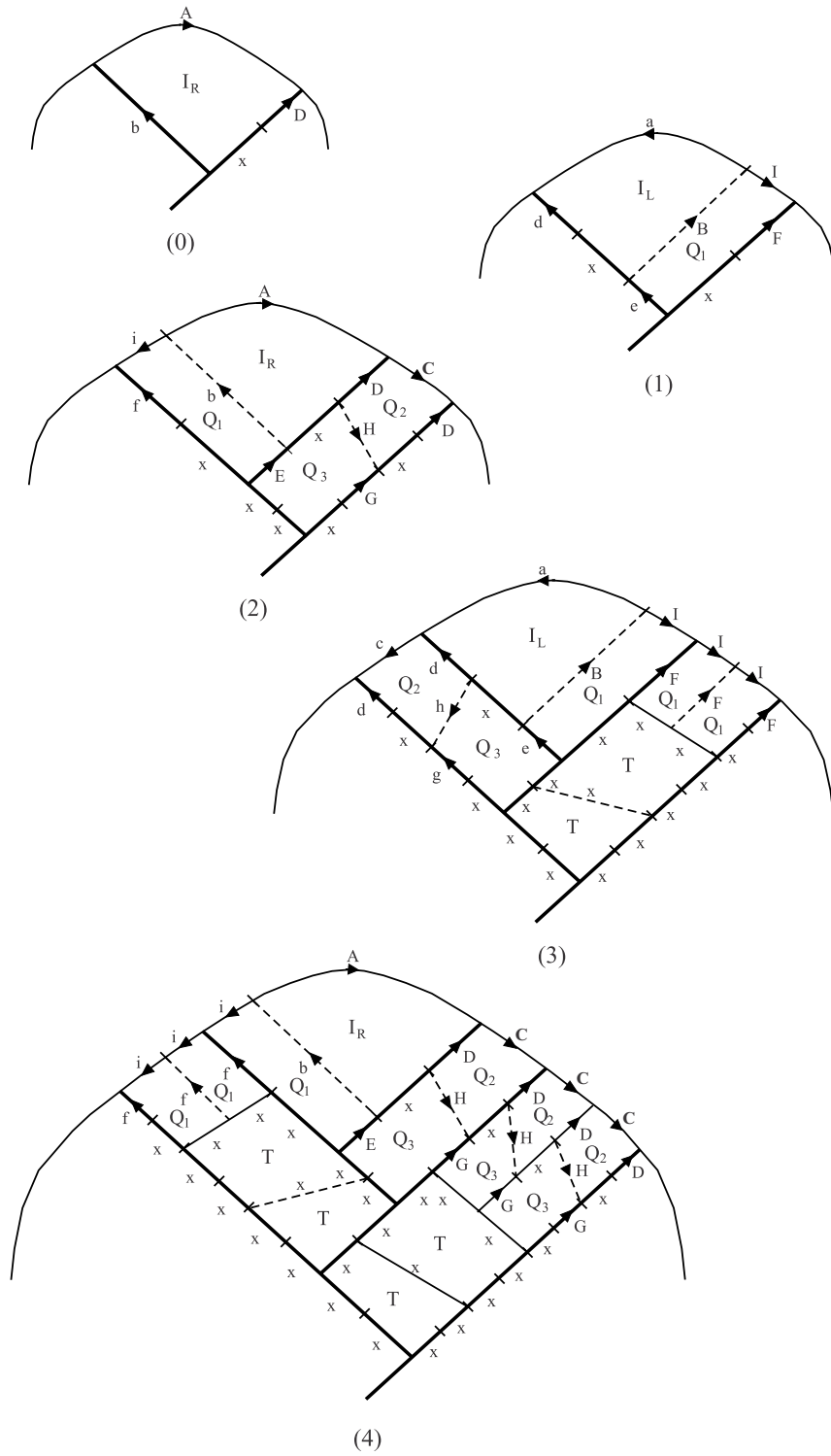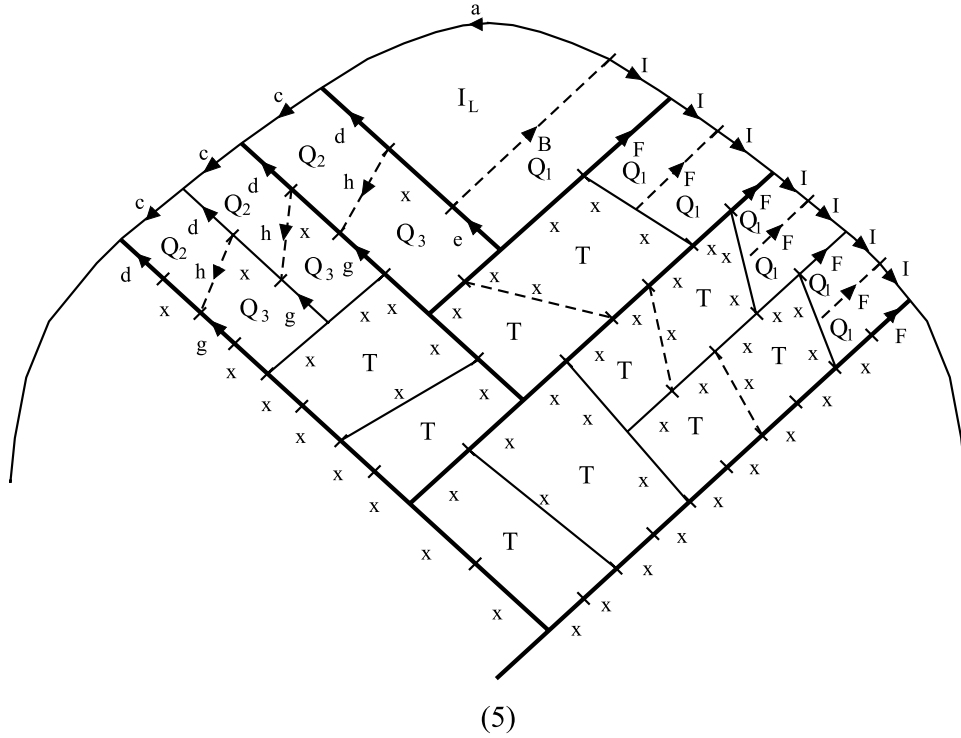
Figure 7.10: Developmental sequence of a *Microsorium* gametophyte

(5)

$$\omega : \ \overrightarrow{A}\,\overleftarrow{D}\,x\,\overrightarrow{b}$$

$l_1:$	$\overrightarrow{a}$	$\rightarrow$	$\overleftarrow{A}\,[+\,\overleftarrow{b}]\,\overrightarrow{i}$		
$l_2:$	$\overrightarrow{b}$	$\rightarrow$	$\overrightarrow{e}\,[-\,\overrightarrow{B}]\,x\,[+\,\overrightarrow{h}]\,\overrightarrow{d}$		
$l_3:$	$\overrightarrow{d}$	$\rightarrow$	$\overrightarrow{f}$		
$l_4:$	$\overrightarrow{f}$	$\rightarrow$	$\overrightarrow{g}\,[-\,\overleftarrow{h}]\,x\,[+\,\overrightarrow{h}]\,\overrightarrow{d}$		
$l_5:$	$\overrightarrow{h}$	$\rightarrow$	$x\,[-\,\overrightarrow{f}]\,x$		
$l_6:$	$\overrightarrow{i}$	$\rightarrow$	$\overrightarrow{c}$		
$l_7:$	$\overrightarrow{c}$	$\rightarrow$	$\overrightarrow{i}\,[+\,\overleftarrow{f}]\,\overrightarrow{i}$		
$l_8:$	$\overrightarrow{e}$	$\rightarrow$	$x\,[+\,x]\,x$		
$l_9:$	$\overrightarrow{g}$	$\rightarrow$	$x\,[-\,x]\,x\,[+\,x]\,x$		

$r_1:$	$\overrightarrow{A}$	$\rightarrow$	$\overleftarrow{a}\,[-\,\overleftarrow{B}]\,\overrightarrow{I}$
$r_2:$	$\overrightarrow{B}$	$\rightarrow$	$\overrightarrow{E}\,[+\,\overrightarrow{b}]\,x\,[-\,\overrightarrow{H}]\,\overrightarrow{D}$
$r_3:$	$\overrightarrow{D}$	$\rightarrow$	$\overrightarrow{F}$
$r_4:$	$\overrightarrow{F}$	$\rightarrow$	$\overrightarrow{G}\,[+\,\overleftarrow{H}]\,x\,[-\,\overrightarrow{H}]\,\overrightarrow{D}$
$r_5:$	$\overrightarrow{H}$	$\rightarrow$	$x\,[+\,\overrightarrow{F}]\,x$
$r_6:$	$\overrightarrow{I}$	$\rightarrow$	$\overrightarrow{C}$
$r_7:$	$\overrightarrow{C}$	$\rightarrow$	$\overrightarrow{I}\,[-\,\overleftarrow{F}]\,\overrightarrow{I}$
$r_8:$	$\overrightarrow{E}$	$\rightarrow$	$x\,[-\,x]\,x$
$r_9:$	$\overrightarrow{G}$	$\rightarrow$	$x\,[+\,x]\,x\,[-\,x]\,x$

Figure 7.10 (continued): Developmental sequence of *Microsorium*

basal cell Q_3 is divided by another periclinal wall into two "terminal"
cells T that do not undergo further divisions. At the same time, the cell
Q_2 lying on the thallus border is divided by an anticlinal wall into two
cells of type Q_1. Each of these cells divides in the same way as the pri-
mary cell. Consequently, the recursive nature of segment development
can be captured by the following cell division system:

$$ Q_1 \rightarrow \frac{Q_2}{Q_3} \qquad\qquad Q_2 \rightarrow Q_1 \mid Q_1 \qquad\qquad Q_3 \rightarrow \frac{T}{T} $$

In the above rules, a horizontal bar denotes a periclinal wall between
cells, and a vertical bar denotes an anticlinal wall.

Development of the thallus

The development of the *Microsorium* thallus is a result of concur-
rent divisions of the apical and segment cells. A single division of the
apical cell corresponds to a single step in segment development. A de-
velopmental sequence that combines the activity of the apex and the
segments is shown in Figure 7.10. This figure also reveals offsets be-
tween neighboring walls. It can be assumed that periclinal division
walls form S-offsets in the segments on the right side of the apex and
Z-offsets in the segments on the left side.

Map L-system

In order to capture the development of *Microsorium* using the for-
malism of map L-systems, it is necessary to identify all combinations
of cells that may lie on both sides of a wall. Careful examination
of these combinations yields the wall labeling scheme shown in Fig-
ure 7.10. Two walls have the same label if and only if they divide in
the same way.[2] The uppercase letters apply to right segment walls, and
the corresponding lowercase letters denote symmetric walls in the left
segments. A comparison of pairs of subsequent structures yields the
L-system in the figure.

Apical cell division results from the application of productions r_1
and l_2 (creation of a right segment) or l_1 and r_2 (creation of a left
segment). Subsequent cell divisions in right and left segments proceed
symmetrically. The development of a right segment is examined in
detail.

The insertion of wall segment B creates the first cell Q_1 of segment
$S_R{}^{(1)}$ (cf. Figure 7.8). Concurrently, wall D on the opposite side of the
segment is transformed into F (step 1). This transformation introduces
a one-step delay before the application of production r_4 which, together
with r_2, splits cell Q_1 into Q_2 and Q_3 by the first periclinal wall H (step
2). As the derivation progresses, production r_4 inserts subsequent per-
iclinal walls H between pairs of anticlinal walls F (step 4). Production

---

[2]It is conceivable to formulate an algorithm that would assign labels consistent
with the above rule automatically. However, the labeling scheme given in Figure 7.10
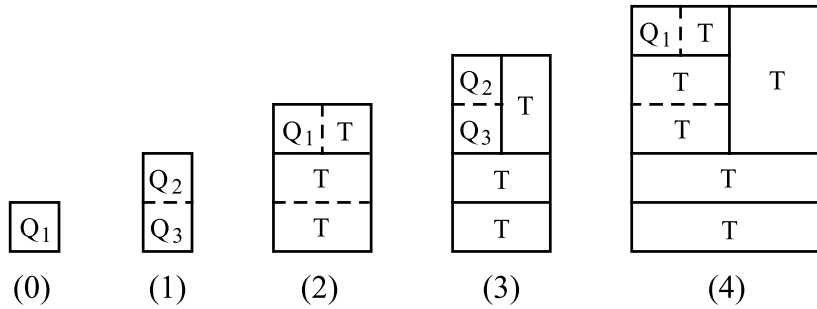was obtained "by hand."

Figure 7.11: Developmental sequence of a basal *Microsorium* segment

r_3 introduces a delay needed to create walls F, which are inserted between periclinal walls H and apical walls I using productions r_5 and r_7. Production r_6 plays a role analogous to r_3 — it introduces a one-step delay into the cycle which creates markers F at the apical front of the segment. Thus, periclinal walls H and anticlinal walls F are produced alternately, in subsequent derivation steps. The last two productions, r_8 and r_9, create terminal walls x that do not undergo further changes. The first such wall is inserted between walls labeled G and E during derivation step 3. The subsequent walls x are inserted every second step between pairs of walls G; only production r_9 is applied in these cases.
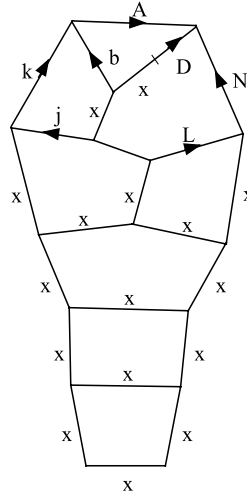
The L-system in Figure 7.10 was formulated under the assumption *Basal segments* that all segments develop in the same way. However, in a real organism the two oldest segments, situated at the thallus base, form a modified pattern with less extensive cell divisions. The developmental sequence of a right basal segment is shown in Figure 7.11. The corresponding cell division system is given below.

$$Q_1 \to \frac{Q_2}{Q_3} \qquad Q_2 \to Q_1 \mid T \qquad Q_3 \to \frac{T}{T}$$

The development of a *Microsorium* gametophyte including basal segments is captured by Figure 7.12. Only productions describing the development of the right side of the thallus are given. Their predecessors are denoted by uppercase letters. The corresponding lowercase productions, which complete the L-system definition, can be obtained by switching the "case" of letters and the orientation of markers. Wall directions remain unchanged. For example, the right-side production

$$r_x: \ \overrightarrow{P} \ \to \ \overleftarrow{A}[-\overrightarrow{b}]C$$

$$
\begin{aligned}
r_1 : \quad & \overrightarrow{A} \;\rightarrow\; \overleftarrow{a}\,[-\;\overleftarrow{B}]\;\overrightarrow{I} \\
r_2 : \quad & \overrightarrow{B} \;\rightarrow\; \overrightarrow{E}\,[+\;\overrightarrow{b}]\;x\,[-\;\overrightarrow{H}]\;\overrightarrow{D} \\
r_3 : \quad & \overrightarrow{D} \;\rightarrow\; [-\;\overrightarrow{M}]\;\overrightarrow{F} \\
r_4 : \quad & \overrightarrow{F} \;\rightarrow\; \overrightarrow{G}\,[+\;\overleftarrow{H}]\;x\,[-\;\overrightarrow{H}]\;\overrightarrow{D} \\
r_5 : \quad & \overrightarrow{H} \;\rightarrow\; x\,[+\;\overrightarrow{F}]\;x \\
r_6 : \quad & \overrightarrow{I} \;\rightarrow\; \overrightarrow{C} \\
r_7 : \quad & \overrightarrow{C} \;\rightarrow\; \overrightarrow{I}\,[-\;\overleftarrow{F}]\;\overrightarrow{I} \\
r_8 : \quad & \overrightarrow{E} \;\rightarrow\; x\,[-\;x]\;x
\end{aligned}
\qquad
\begin{aligned}
r_9 : \quad & \overrightarrow{G} \;\rightarrow\; x\,[+\;x]\;x\,[-\;x]\;x \\
r_{10} : \quad & \overrightarrow{J} \;\rightarrow\; \overrightarrow{L} \\
r_{11} : \quad & \overrightarrow{K} \;\rightarrow\; \overrightarrow{N} \\
r_{12} : \quad & \overrightarrow{L} \;\rightarrow\; x\,[+\;\overleftarrow{M}]\;x \\
r_{13} : \quad & \overrightarrow{M} \;\rightarrow\; x\,[+\;\overrightarrow{L}]\;x \\
r_{14} : \quad & \overrightarrow{N} \;\rightarrow\; \overrightarrow{O} \\
r_{15} : \quad & \overrightarrow{O} \;\rightarrow\; x\,[+\;\overleftarrow{L}]\;\overrightarrow{N}
\end{aligned}
$$

Figure 7.12: The initial map and productions for the right side of a *Microsorium linguaeforme* with basal segments

corresponds to the left-side production

$$
l_x : \quad \overrightarrow{p} \;\rightarrow\; \overleftarrow{a}[+\overrightarrow{B}]c.
$$

Additional examples can be found by comparing the left and right columns of the L-system in Figure 7.10.

Assuming the starting map specified by Figure 7.12, a simulated developmental sequence interpreted using the dynamic method to determine cell shape is given in Figure 7.13. Different colors are used to indicate the apical cell, the alternating "regular" segments, and the basal segments. A comparison of the last developmental stage with a photograph of a real gametophyte (Figure 7.14) shows good correspondence between the model and reality with respect to structure topology, the relative sizes and shapes of cells, and the overall shape of the thallus. This result is particularly interesting from a biological perspective, since it indicates that genetically controlled cell division patterns play an important role in determining the shape of a structure.
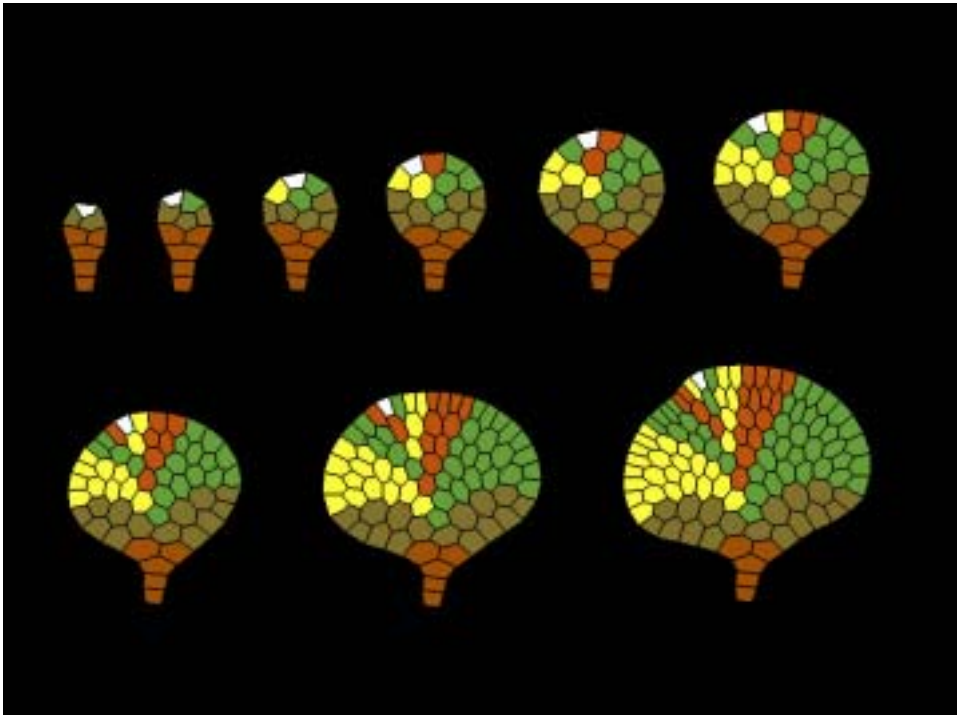
Model validation

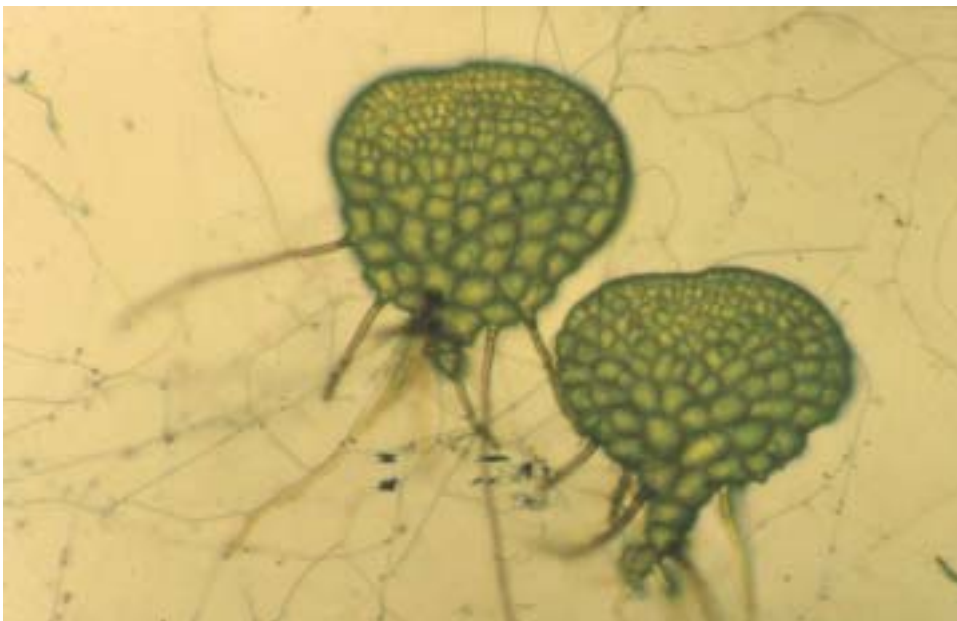Figure 7.13: Simulated development of *Microsorium linguaeforme*

Figure 7.14: Microphotograph of *Microsorium linguaeforme* at magnification 70x
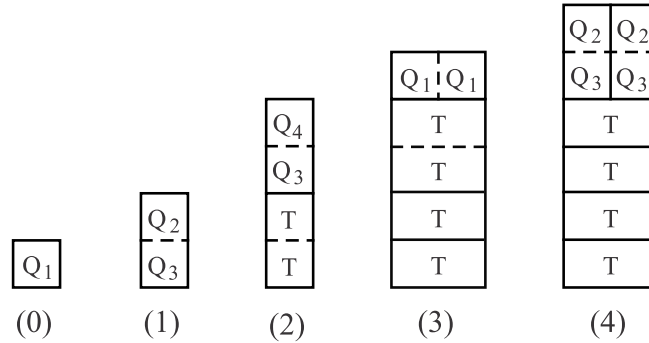
Figure 7.15: Developmental sequence of a *Dryopteris* segment

7.4   Dryopteris thelypteris

Gametophytes of other fern species follow a similar developmental pattern, with the apex producing segments alternately to the left and right. However, the cell division patterns within segments vary between species yielding different thalli shapes. For example, Figure 7.15 shows segment development in *Dryopteris thelypteris*. The corresponding cell division system is given below.

$$Q_1 \rightarrow \frac{Q_2}{Q_3} \qquad Q_2 \rightarrow \frac{Q_4}{Q_3} \qquad Q_3 \rightarrow \frac{T}{T} \qquad Q_4 \rightarrow Q_1 \mid Q_1$$

A developmental cycle of length 3, starting at cell Q_1, produces two new cells Q_1 separated by an anticlinal wall and a sequence of four terminal cells T separated by periclinal walls. A developmental sequence that combines the activity of the apex and the segments is shown in Figure 7.17. As in the case of the map L-system in Figure 7.12, only productions for the right side of the thallus are shown.

Map L-system   Apical cell division results from the application of productions r_1 and l_2 (creation of a right segment) or l_1 and r_2 (creation of a left segment). The subsequent cell divisions proceed in a symmetric way in right and left segments. The development of a right segment is described below.

The insertion of wall segment B creates the first cell Q_1 of segment $S_R{}^{(1)}$ (cf. Figure 7.8). Concurrently, wall D on the opposite side of the segment is transformed by production r_6 into FG (step 1). This transformation introduces a one-step delay before the application of production r_7 which, together with r_2, splits cell Q_1 into Q_2 and Q_3 by the first periclinal wall x (step 2). Meanwhile, production r_3 replaces wall C by wall J (step 1), after which r_4 replaces J by E (step 2). This introduces a two-step delay before cell Q_3 is subdivided periclinally into two cells T by production r_5 (step 3). In the same step, productions r_6 and r_9 subdivide cell Q_2 into cells Q_3 and Q_4, separated by periclinal wall H. Wall O from step 1 is transformed into wall R by productions
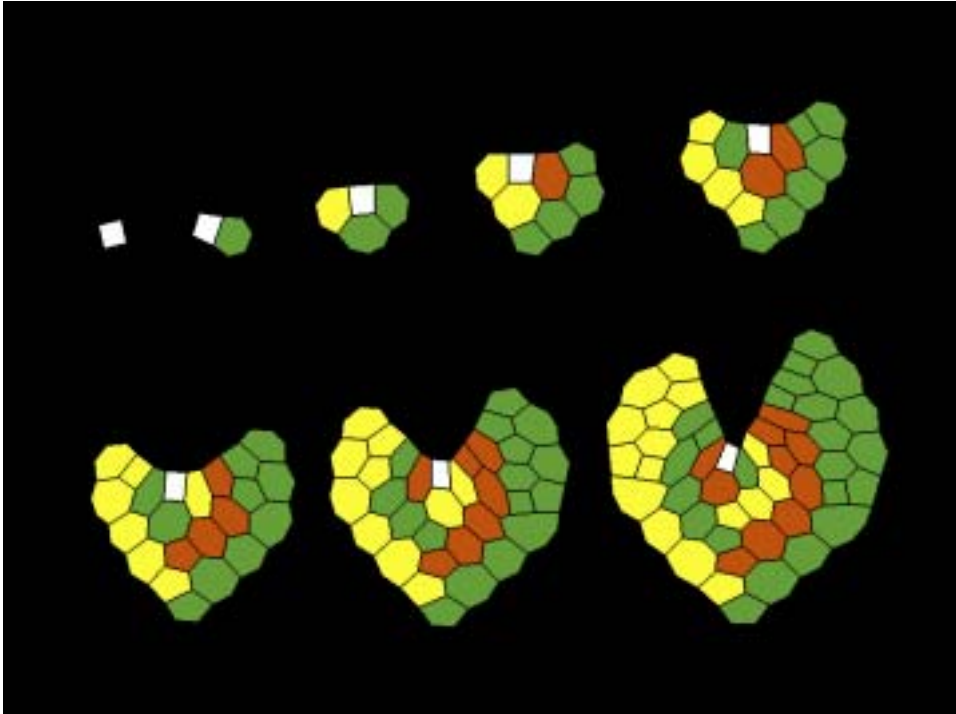
Figure 7.16: Simulated development of *Dryopteris thelypteris*

r_{15} (step 2) and r_{16} (step 3). Walls R and H are replaced by r_{17} and r_{14}, resulting in the first anticlinal division of cell Q_4 into two cells Q_1 by wall I (step 4). At the same time, productions r_5 and r_6 split cell Q_3 periclinally into two cells T. In the following derivation steps, each of the newly created cells Q_1 undergoes a sequence of changes similar to that described above. Production r_8 introduces a one-step delay before Q_1 is subdivided into Q_2 and Q_3 using r_9 and r_{10} (analogous to r_2 and r_7). Productions r_{11} and r_{12} play a role similar to r_5 and r_6, while production r_{13} introduces a delay. Walls labeled x do not undergo further changes and cells T do not subdivide. A simulated developmental sequence generated by the L-system in Figure 7.17 using the dynamic method to determine cell shape is given in Figure 7.16.

A comparison of *Microsorium* and *Dryopteris* gametophytes (either real or modeled) indicates that different division patterns of segment cells have a large impact on the overall thalli shapes. In *Microsorium*, the number of *marginal cells*, situated at the apical front of a segment, is doubled every second derivation step. The segments are approximately triangular, with a wide apical front, which results in the circular thallus shape. The apical front of *Dryopteris* segments is comparatively less developed. The number of marginal cells is doubled only every third step, and the segments grow faster in length. The resulting thallus shape is concave.
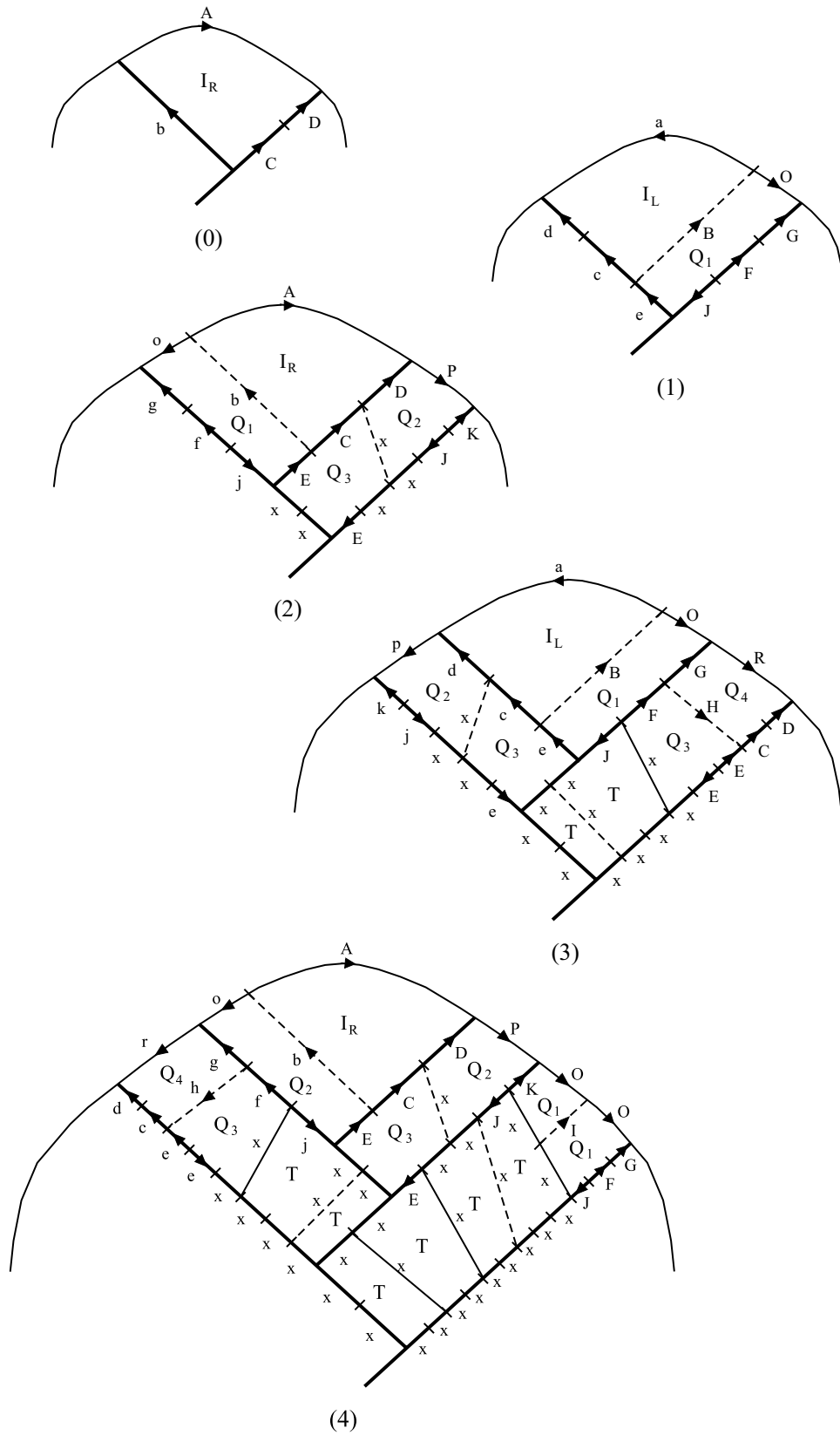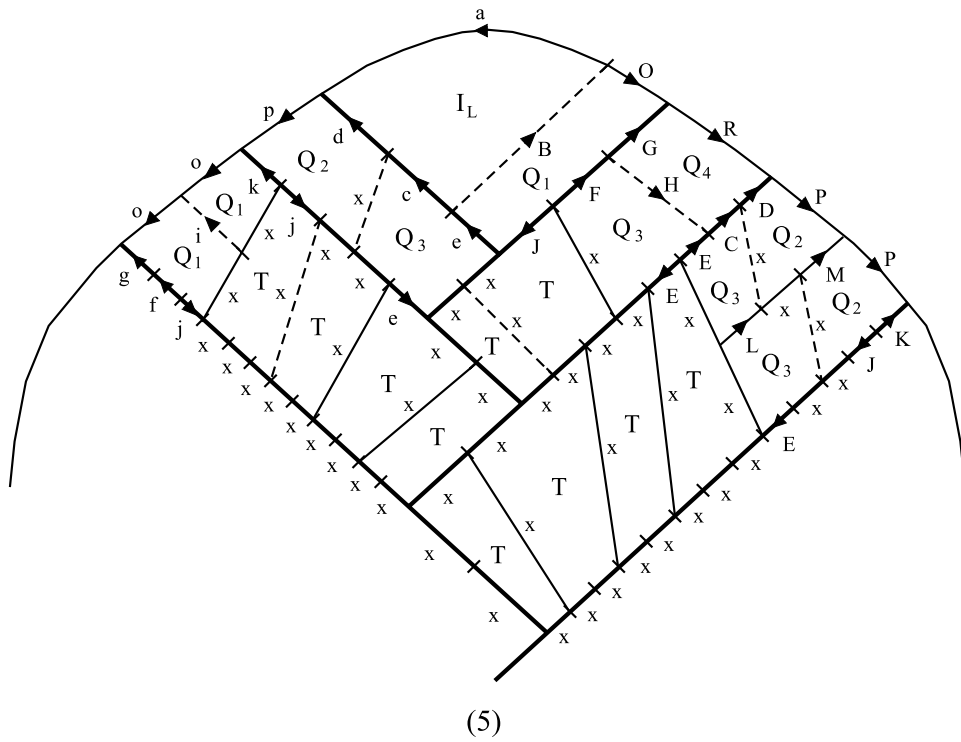
Microsorium vs. Dryopteris

Figure 7.17: Developmental sequence of a *Dryopteris* gametophyte

(5)

ω : $\overrightarrow{A}\overleftarrow{D}\overleftarrow{C}\overrightarrow{b}$

r_1 : $\overrightarrow{A}$ $\rightarrow$ $\overleftarrow{a}\left[-\overleftarrow{B}\right]\overrightarrow{O}$

r_2 : $\overrightarrow{B}$ $\rightarrow$ $\overrightarrow{E}\left[+\overrightarrow{b}\right]\overleftarrow{C}\left[-x\right]\overrightarrow{D}$

r_3 : $\overrightarrow{C}$ $\rightarrow$ $\overleftarrow{J}$

r_4 : $\overrightarrow{J}$ $\rightarrow$ $\overrightarrow{E}$

r_5 : $\overrightarrow{E}$ $\rightarrow$ $x\left[-x\right]x$

r_6 : $\overrightarrow{D}$ $\rightarrow$ $\overrightarrow{F}\left[-\overrightarrow{H}\right]\overrightarrow{G}$

r_7 : $\overrightarrow{F}$ $\rightarrow$ $x\left[+x\right]x\left[-x\right]\overleftarrow{J}$

r_8 : $\overrightarrow{G}$ $\rightarrow$ $\overrightarrow{K}$

r_9 : $\overrightarrow{K}$ $\rightarrow$ $\overrightarrow{E}\left[+\overrightarrow{H}\right]\overleftarrow{C}\left[-x\right]\overrightarrow{D}$

r_{10} : $\overrightarrow{I}$ $\rightarrow$ $\overrightarrow{L}\left[+x\right]x\left[-x\right]\overrightarrow{M}$

r_{11} : $\overrightarrow{L}$ $\rightarrow$ $x\left[+x\right]x\left[-x\right]x$

r_{12} : $\overrightarrow{M}$ $\rightarrow$ $\overrightarrow{L}\left[+\overleftarrow{H}\right]x\left[-\overrightarrow{H}\right]\overrightarrow{N}$

r_{13} : $\overrightarrow{N}$ $\rightarrow$ $\overrightarrow{I}$

r_{14} : $\overrightarrow{H}$ $\rightarrow$ $x\left[+\overrightarrow{I}\right]x$

r_{15} : $\overrightarrow{O}$ $\rightarrow$ $\overrightarrow{P}$

r_{16} : $\overrightarrow{P}$ $\rightarrow$ $\overrightarrow{Q}$

r_{17} : $\overrightarrow{Q}$ $\rightarrow$ $\overrightarrow{O}\left[-\overleftarrow{I}\right]\overrightarrow{O}$

Figure 7.17 (continued): Developmental sequence of *Dryopteris*

In order to quantify the relationship between segment cell division pattern and thallus shape, de Boer [22] proposed an empirical measure called *periclinal ratio*. It is based on the following considerations:

- anticlinal growth takes place mainly along the margin and is exponential since all marginal cells divide; and

- periclinal growth of a segment is linear, as cells displaced away from the margin eventually stop dividing.

Since the division pattern is recursive, the average ratio of the numbers of marginal cells in neighboring segments converges to a constant A. Similarly, the difference between the numbers of cells along the periclinal boundary of two neighboring segments converges to a constant P. By computer simulation [22], it was found that if the periclinal ratio P/A is smaller than 1.25, the apical front is convex as in the case of *Microsorium linguaeforme*. In contrast, if P/A is larger than 2.0, the simulated structure develops a concave apical front, corresponding to a heart-shaped thallus as in *Dryopteris thelypteris*. These results relate local growth to global shape. Periclinal ratios from 1.25 to 2.0 were not studied in detail.

## 7.5   Modeling spherical cell layers

Although the scope of this book is limited to plants, it is interesting to note that the formalism of L-systems can be applied also to simulate some developmental processes in animals. For example, during the *Animal embryos* *cleavage* stage of development, an animal embryo consists of a single layer of cells that covers the surface of a spherical cavity. This structure is known as the *blastula* [6]. The cells divide synchronously in a regular pattern up to and including the 64-cell stage (6th cleavage). This development can be captured using an mBPMOL-system operating on the surface of a sphere rather than on a plane. To this end, cell walls are represented as great circle arcs connecting vertices that are constrained to the sphere surface.

The extension of the dynamic interpretation method from the plane to the surface of a sphere requires few changes. Osmotic pressure and wall tension are calculated as before. Since the resulting force may displace a vertex away from the surface of the sphere, the actual vertex position is found by projecting the displaced point back to the sphere. During the cleavage stage, cells of embryos do not expand, thus the overall size of the sphere is constant.

Patella vulgata   For example, deBoer [22] proposed the map L-system in Figure 7.18 to model the development of a snail embryo, *Patella vulgata*, according to data presented by Biggelaar [150]. The starting map and developmental sequence are shown in Figure 7.18, while Figure 7.19 presents an alternative rendering. Each cell is approximated by a sphere centered at the point obtained by raising the center of gravity of the cell
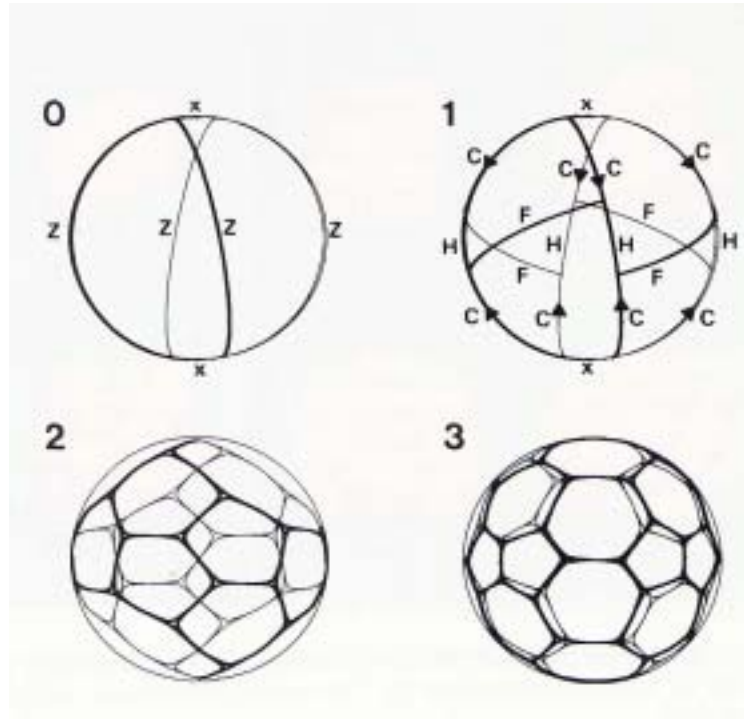
$$
\begin{aligned}
p_1 &: & \texttt{A} &\;\rightarrow\; \texttt{b[-a]x[+a]b} \\
p_2 &: & \texttt{a} &\;\rightarrow\; \texttt{B[+A]x[-A]B} \\
p_3 &: & \texttt{B} &\;\rightarrow\; \texttt{a} \\
p_4 &: & \texttt{b} &\;\rightarrow\; \texttt{A} \\
p_5 &: & \overrightarrow{\texttt{C}} &\;\rightarrow\; \overrightarrow{\texttt{D}}\,\texttt{[+a]}\,\overrightarrow{\texttt{E}} \\
p_6 &: & \overrightarrow{\texttt{D}} &\;\rightarrow\; \overrightarrow{\texttt{C}}\,\texttt{[-A]x} \\
p_7 &: & \overrightarrow{\texttt{E}} &\;\rightarrow\; \overrightarrow{\texttt{C}} \\
p_8 &: & \texttt{F} &\;\rightarrow\; \overleftarrow{\texttt{E}}\,\texttt{[-a]G[+a]}\,\overrightarrow{\texttt{E}} \\
p_9 &: & \texttt{G} &\;\rightarrow\; \texttt{J} \\
p_{10} &: & \texttt{H} &\;\rightarrow\; \texttt{I} \\
p_{11} &: & \texttt{I} &\;\rightarrow\; \texttt{B[-A]x[+A]B} \\
p_{12} &: & \texttt{J} &\;\rightarrow\; \texttt{b[+a]x[-a]b} \\
p_{13} &: & \texttt{Z} &\;\rightarrow\; \overrightarrow{\texttt{C}}\,\texttt{[-F]H[+F]}\,\overleftarrow{\texttt{C}}
\end{aligned}
$$

Figure 7.18: Developmental sequence of *Patella vulgata* (equatorial view)

vertices to the surface of the underlying spherical cavity. The radius is the maximum distance from the center of gravity to the cell vertices. A comparison of the *Patella* model at the 16-cell stage (bottom left of Figure 7.19) with an electron microscope image (Figure 7.20) shows good correspondence between the model and reality.

7.6   Modeling 3D cellular structures

Cellworks   The previous sections presented a method for modeling cellular layers extending in a plane or on the surface of a sphere. However, real cellular structures are three-dimensional objects. In order to capture the three-dimensional aspect of cellular layers and model more complex structures, Lindenmayer [85] proposed an extension of map L-systems called *cellwork* L-systems. The notion of a cellwork is characterized as follows.

- A cellwork is a finite set of *cells*. Each cell is surrounded by one or more *walls* (faces).

- Each wall is surrounded by a boundary consisting of a finite, circular sequence of *edges* that meet at *vertices*.

- Walls cannot intersect without forming an edge, although there can be walls without edges (in the case of cells shaped as spheres or tori).

- Every wall is part of the boundary of a cell, and the set of walls is connected.

- Each edge has one or two vertices associated with it. The edges cannot cross without forming a vertex, and there are no vertices without an associated edge.

- Every edge is a part of the boundary of a wall, and the set of edges is connected.

Note that the terms *cell* and *wall* have different meanings in the context of cellworks than in the context of maps.

mBPCOL-system   The development of three-dimensional structures is captured using an extension of mBPMOL-systems called *marker Binary Propagating Cellwork OL-systems* [42]. An mBPCOL-system $\mathcal{G}$ is defined by a finite alphabet of *edge labels* Σ, a finite alphabet of *wall labels* Γ, a *starting cellwork* ω, and a finite set of *edge productions* P. The initial cellwork ω is specified by a list of walls and their bounding edges. As in the case of mBPMOL-systems, edges may be directed or neutral. Each production is of the form $A : \beta \to \alpha$, where the edge $A \in \Sigma$ is the *predecessor*, the string $\beta \in \{\Gamma^+, *\}$ is a list of *applicable walls* (* denotes all walls), and the string α is the *successor*, which is composed of edge labels from Σ,
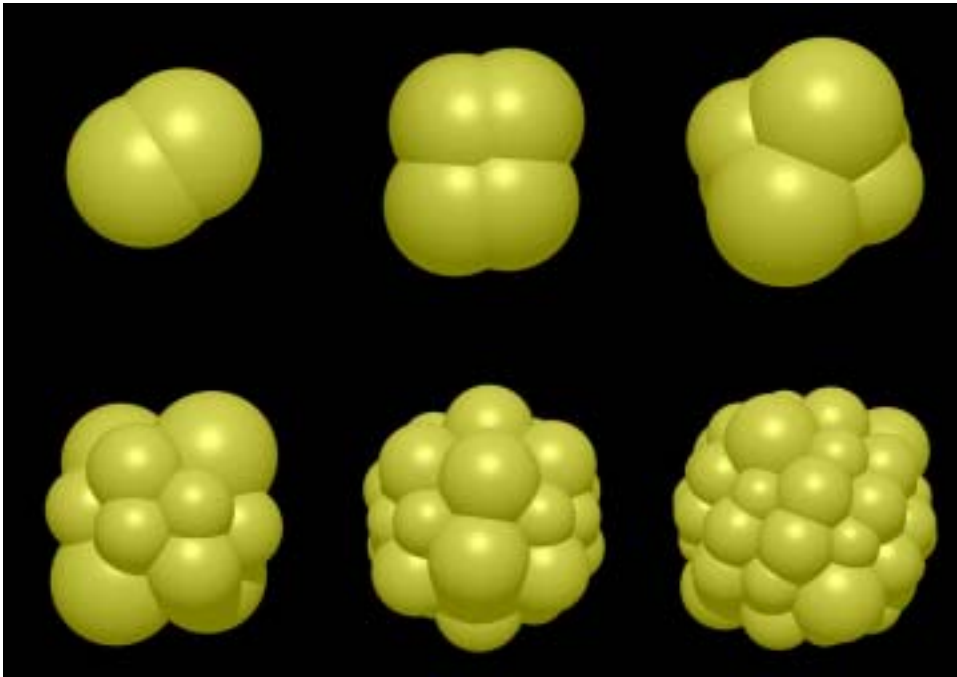
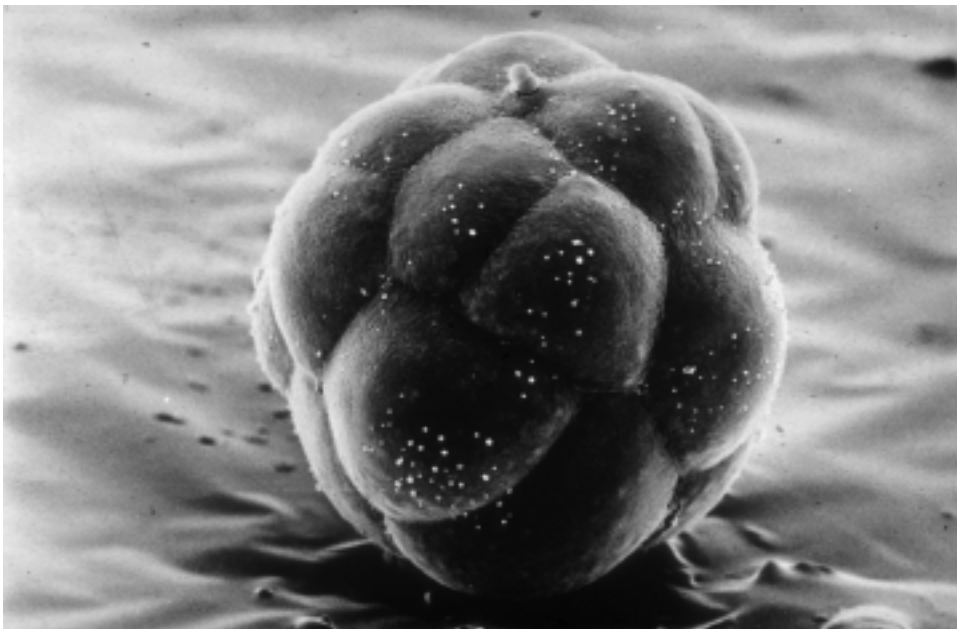Figure 7.19: Simulated development of *Patella vulgata*

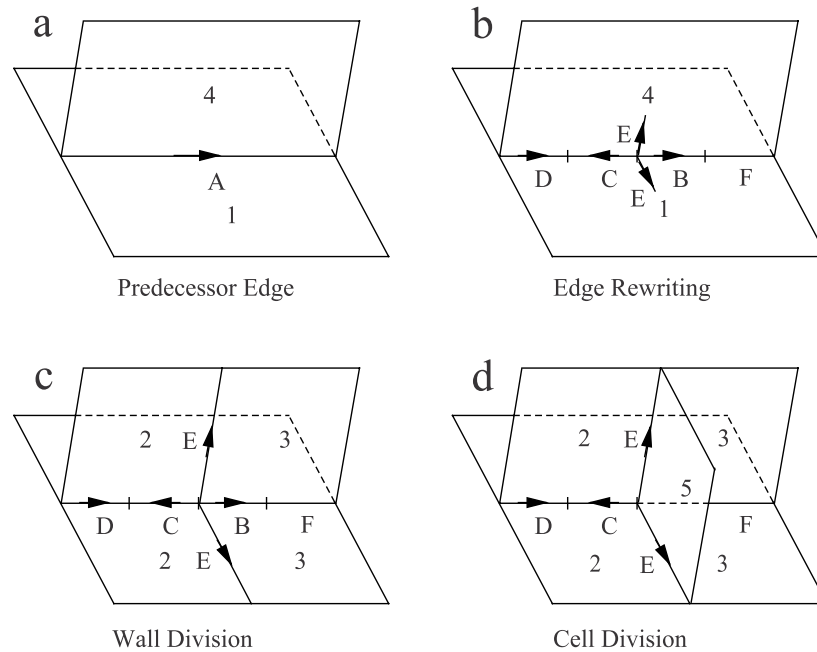Figure 7.20: An electron microscope image of *Patella vulgata*

Figure 7.21: The phases of a derivation step

wall labels from Γ and the symbols [and]. The symbols outside square brackets describe the subdivision pattern for the predecessor. Pairs of matching brackets [and] delimit *markers* that specify possible attachment sites for new edges and walls. As in the two-dimensional case, arrows indicate the relative directions of successor edges and markers with respect to the predecessor edge. The list β contains all walls into which a marker should be inserted. In addition to the labels for edges and markers, a production successor specifies the labels of walls that may be created as a result of a derivation step.

Production syntax
    The syntax of a production is best explained using an example. The production

$$\vec{A} : 14 \rightarrow \vec{D}\overleftarrow{C}_2[\vec{E}_5]\vec{B}_3 F$$

applies to an edge A if it belongs to one or more walls labeled 1 or 4 (Figure 7.21a). The predecessor edge is subdivided into four edges D, C, B and F. During a derivation step, marker E is introduced into all walls of type 1 or 4 that share edge A (Figure 7.21b), and can be connected with a matching marker inserted into the same wall by another production. As a result, the wall will split into two. The daughter wall having C as one of its edges will be labeled 2, and the wall having B as an edge will be labeled 3 (Figure 7.21c). Markers E can be connected only if both productions assign labels to the daughter walls in a consistent way. Otherwise, the markers are considered non-matching and are discarded. If several walls bounding a cell split in such a way that the sequence of new edges forms a closed contour, a
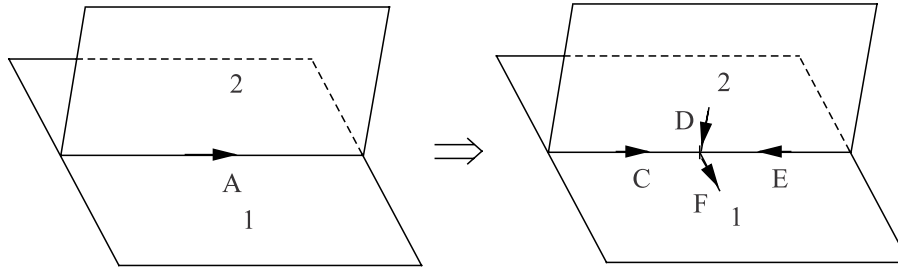
Figure 7.22: Example of consistent edge productions

new wall bound by these edges may be created. In order for this to occur, all markers involved must specify the same label for the new wall, 5 in this example (Figure 7.21d).

The limitation of the scope of a production to specific walls may create a consistency problem while rewriting edges. For instance, assume that walls 1 and 2 share edge A and the following productions are in P:

$$p_1 : \quad \overrightarrow{A} : 1 \quad \rightarrow \quad \overrightarrow{C}\overleftarrow{E}$$
$$p_2 : \quad \overrightarrow{A} : 2 \quad \rightarrow \quad \overrightarrow{A}\overrightarrow{B}$$

Productions p_1 and p_2 are inconsistent since they specify two different partitions of the same edge. It is assumed that the mBPCOL-systems under consideration are free of such inconsistencies. This does not preclude the possibility of applying several productions simultaneously to the same edge. For example, a production pair,

$$p_1 : \quad \overrightarrow{A} : 1 \quad \rightarrow \quad \overrightarrow{C}_2[\overrightarrow{F}_3]\overleftarrow{E}_4$$
$$p_2 : \quad \overrightarrow{A} : 2 \quad \rightarrow \quad \overrightarrow{C}_5[\overleftarrow{D}_6]\overleftarrow{E}_7,$$

consistently divides edge A into segments C and E, although the markers inserted into walls 1 and 2 are different (Figure 7.22).

According to the above discussion, a *derivation step* in an mBPCOL-system consists of three phases.   *Derivation*

- Each edge in the cellwork is replaced by successor edges and markers using one or more productions in P.

- Each wall is scanned for matching markers. If a match inducing a consistent labeling of daughter cells is found, the wall is subdivided. The selection of matching markers is done by the system. Unused markers are discarded.

- Each cell is scanned for a circular sequence of new division edges. If a cycle assigning the same label to the division wall is found, it is used to bound the wall that will divide the cell into two daughter cells. If different possibilities exist, the edges are selected by the system.

$$p_1 \; : \quad \text{A} \; : \; 1 \quad \rightarrow \quad \text{B}_1\big[\text{A}_2\big]\text{B}_1$$
$$p_2 \; : \quad \text{A} \; : \; 2 \quad \rightarrow \quad \text{B}_2\big[\text{C}_2\big]\text{B}_2$$
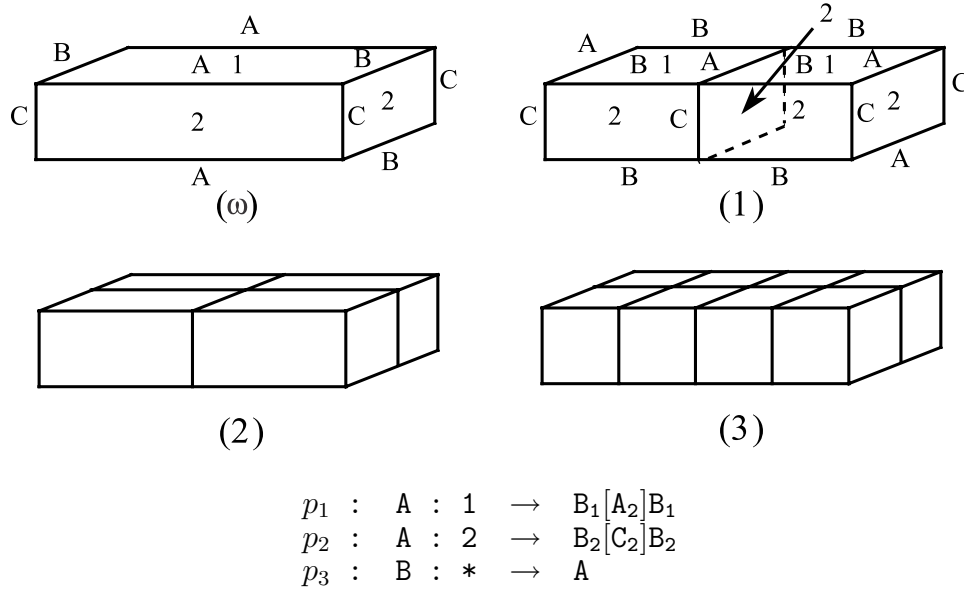$$p_3 \; : \quad \text{B} \; : \; * \quad \rightarrow \quad \text{A}$$

Figure 7.23: Example of a cellwork L-system

A wall may be subdivided more than once as long as new division edges do not intersect and a consistent labeling of daughter walls is possible. In contrast, a cell may be divided only once in any derivation step.

Example   For example, Figure 7.23 presents a three-dimensional extension of the map L-system from Figure 7.2. In the first derivation step, production p_1 divides walls labeled 1, and production p_2 divides walls labeled 2. The inserted edges form a cycle that divides the cell with a new wall labeled 2. In the subsequent steps this process is repeated, generating a pattern of alternating division walls. Production p_3 introduces the necessary delay.

Dynamic   The dynamic method for interpreting map L-systems is extended to
interpretation   cellwork L-systems using the following assumptions:

- the structure is represented as a three-dimensional network of masses corresponding to cell vertices, connected by springs which correspond to cell edges,

- the springs are always straight and obey Hooke's law,

- for the purpose of force calculations, walls can be approximated by flat polygons,

- the cells exert pressure on their bounding walls; the pressure on a wall is directly proportional to the wall area and inversely proportional to the cell volume,

- the pressure on a wall is divided evenly between the wall vertices,

- the motion of masses is damped, and

- other forces are not considered.

The total force $\vec{F}_T$ acting on a vertex X is given by the formula

$$\vec{F}_T = \sum_{e \in E} \vec{F}_e + \sum_{w \in W} \vec{F}_w + \vec{F}_d,$$

where $\vec{F}_e$ are forces contributed by the set of edges E incident to X, $\vec{F}_w$ are forces contributed by the set of walls W incident to X, and $\vec{F}_d = -b\vec{v}$ is a damping force. The forces $\vec{F}_e$ act along the cell edges and represent wall *tension*. The forces $\vec{F}_w$ are due to the *pressure* exerted by the cells on their bounding walls. The total force of pressure $\vec{P}$ exerted by a cell on a wall w has direction normal to w and is equal to $p \cdot A$, where p is the internal cell pressure and A is the wall area. Calculation of the polygon area proceeds as in the two-dimensional case. The pressure p is assumed to be inversely proportional to the cell volume, $p \sim V^{-1}$, which corresponds to the equation describing osmotic pressure (Section 7.2). The volume V of a cell is calculated by tesselating the cell into tetrahedra. The resulting differential equations are formed and solved as in the two-dimensional case.

A division pattern that frequently occurs in epidermal cell structures *Epidermal cells* is described by the L-system in Figure 7.24, based on a cyclic cellwork L-system (a slightly different formalism) proposed by Lindenmayer [85]. Productions p_1, p_2, p_6 and p_7 are responsible for cell divisions, while the remaining productions introduce delays such that the division pattern is staggered.

On the surface, the cellular structures analyzed in this chapter may appear quite unrelated to the models discussed previously. However, a closer inspection reveals many analogies. For example, consecutively created segments of a fern gametophyte exhibit a phase effect corresponding to that observed in inflorescences. Furthermore, parts of an older gametophyte situated near the apex have the same topology as the entire thallus at an earlier developmental stage, which associates the recursive structures generated by map or cellwork L-systems with self-similar patterns created using string L-systems. As observed by Oppenheimer [105], self-similarity appears to be one of the general principles organizing the world of botany. The next chapter discusses this topic in more detail.

a

b

c

d

e

f

g

$$
\begin{array}{llll}
p_1: & \text{A}:123 & \rightarrow & \text{C}_3[\text{E}_1]\text{B}_2[\text{D}_1]\text{C}_3 \\
p_2: & \text{A}:4 & \rightarrow & \text{CB}_4[\text{F}_1]\text{C}_4 \\
p_3: & \text{B}:* & \rightarrow & \text{A} \\
p_4: & \text{C}:* & \rightarrow & \text{B} \\
p_5: & \text{E}:* & \rightarrow & \text{D} \\
p_6: & \text{F}:123 & \rightarrow & \text{HGH} \\
p_7: & \text{F}:4 & \rightarrow & \text{H}_4[\text{F}_1]\text{G}_4[\text{F}_1]\text{H}_4 \\
p_8: & \text{G}:* & \rightarrow & \text{F} \\
p_9: & \text{H}:* & \rightarrow & \text{G}
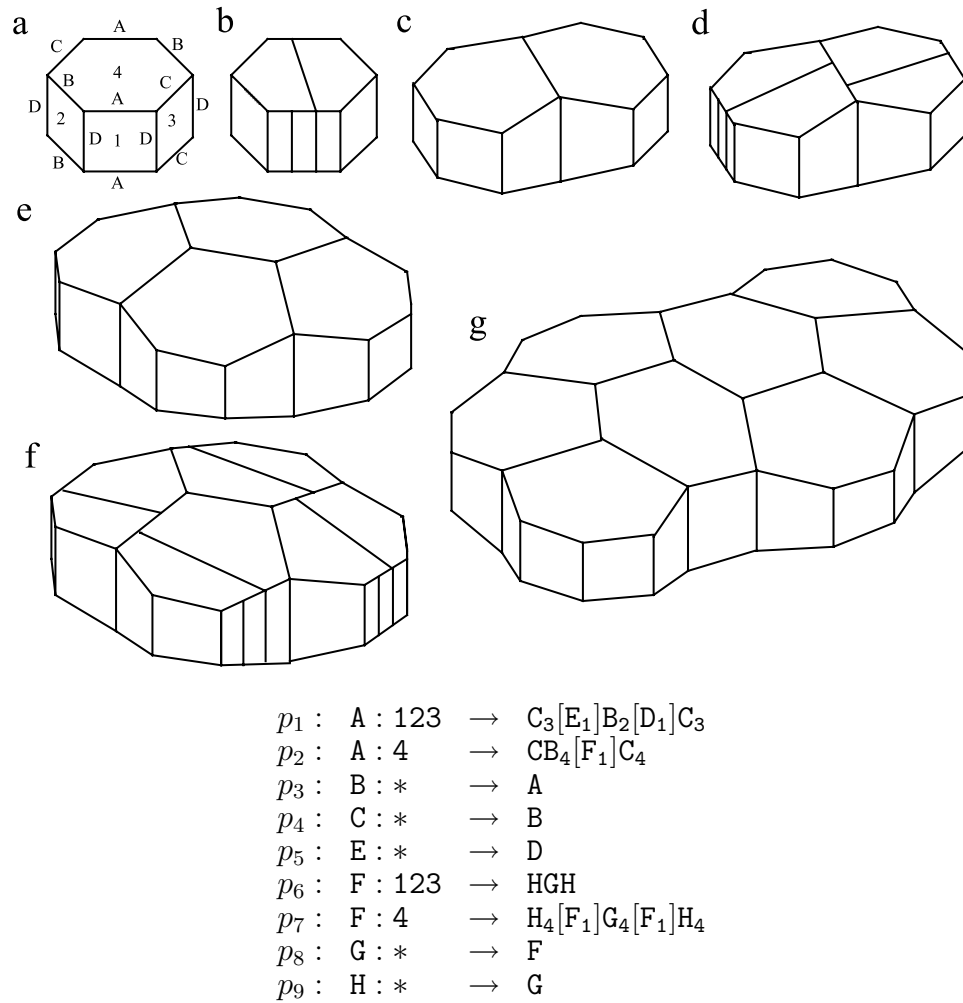\end{array}
$$

Figure 7.24: Developmental sequence of epidermal cells: (a) The starting cellwork; (b), (d) and (f) cellworks immediately after cell divisions; (c), (e) and (g) the corresponding cellworks at equilibrium